Journal of the European Ceramic Society 20 (2000) 1277–1288

TEM characterisation of PZT films prepared by a diol route on platinised silicon substrates

D. Kaewchinda, T. Chairaungsri, M. Naksata, S.J. Milne, R. Brydson*

Department of Materials, School of Process, Environmental and Materials Engineering, University of Leeds, Leeds LS2 9JT, UK

Received 18 January 1999; received in revised form 15 October 1999; accepted 25 October 1999

Abstract

PZT (65/35) films were prepared using a diol route with 10 mol% excess Pb and deposited on $Pt/Ti/SiO_2/Si$ substrates. Samples were characterised using XRD and cross-sectional TEM/STEM in combination with EDX and EELS. Linescan and point analyses were used to investigate the interdiffusion of elements over nanometre length scales during film heat treatments. During annealing at ca. 500°C, significant diffusion of elements occurred which had a dramatic effect on the film characteristics; interdiffusion of Pb and Si were clearly evident and the diffusion and reaction of Pb with the Pt electrode resulted in the formation of a distinct $PbPt_x$ phase ($x = 3$–4) at the film/Pt interface. Drastic interdiffusion of all elements except Zr was detected at higher temperatures; further diffusion of Pb to the underlying layers resulted in a Pb-deficient condition in the bulk film and the formation of a fluorite-type nanocrystalline phase.

Keywords: Annealing; EELS; Electron microscopy; Interdiffusion; Interphase; Pyrochlore; PZT

1. Introduction

In recent years, the wide range of potential applications for integrated lead zirconium titanate, $PbZr_xTi_{(1-x)}O_3$ (PZT), thin films deposited on Si-based microelectronic devices has stimulated considerable interest in the cost-effective fabrication of such films. Sol–gel methods are one such route for thin film production which involves the deposition of an amorphous gel film which is subsequently transformed to a crystalline phase on annealing. These methods have a number of benefits, including high purity, large area of deposition and potentially easy control of composition; however, the resultant microstructure, texture and ferroelectric properties of such films depend on a wide range of parameters including: the film composition, the heating rate, the drying conditions and the annealing temperature.

The crystallisation of sol–gel derived PZT thin films normally requires temperatures above 500°C, hence for processing on silicon substrates, electrically conducting barrier layers are required to avoid reactions between the film and substrate which would degrade film properties.[1] For PZT thin films, the most common electrode-substrate configuration employed is $Pt(111)/Ti/SiO_2/Si$ in which Ti serves as an adhesion and additional buffer layer which is designed to inhibit the diffusion of Si into Pt to form platinum silicides and hence loss of integrity of the Pt electrode.[2–4] The (111) orientation of the Pt layer is generally considered to promote (111) orientation in PZT films due to epitaxial nucleation and growth.[5]

However, interdiffusion of the film and the Pt/Ti metallisation layer has been observed. Chen and Chen[6] and Atsuki[7] have both reported that diffusion of Pb into the underlying layers was a major cause of Pb losses in the Pb-based film resulting in the formation of Pb-deficient pyrochlore or fluorite intermediate phases. Loss of Pb from the film due to volatilisation also promotes the formation of these intermediate phases at the film–air interface.[8] The diffusion of Pb from the PZT film into the Pt electrode has been reported under certain conditions to form a $PbPt_x$ ($x = 5$–7) phase which is epitaxial with the (111) Pt layer and has a closer lattice match to PZT than does Pt[9,10] and therefore provides a major contribution to (111) preferred orientation of PZT films on Pt electrodes.[6]

* Corresponding author. Tel.: +44-113-233-2369; fax: +44-113-242-2531.

E-mail address: mtlrmdb@leeds.ac.uk (R. Brydson).

0955-2219/00/$ - see front matter
PII: S0955-2219(99)00296-4

Diffusion of Ti into the Pt layer has also been reported.[7,11] Atsuki et al.[7] have reported that Ti diffuses to the top surface of the platinum layer and oxidises to form a TiO_x phase during the substrate pre-annealing process. They postulate that the TiO_x phase then reacts with Pb to form a $PbTiO_3$ buffer layer. However, Tani et al.[11] have suggested that outward diffusion and reaction of Ti with the Pt electrode gives rise to the formation of a Pt_3Ti alloy which has a simple cubic structure and a (111) d-spacing which differs from PZT by ca. 0.5%, a similar lattice match to that of $PbPt_{5-7}$. They argue that formation of the Pt_3Ti compound would lead to a reduction in the interfacial energy between electrode and PZT (111) planes, thus assisting the heteroepitaxial nucleation and growth of (111) PZT.

Thus, from these previous studies, it appears that the diffusion of both the film and substrate elements plays an important role, not only in the degradation of film properties, but also in the introduction of a preferred orientation in PZT films. With advances in high spatial resolution microanalytical techniques, it is timely to investigate quantitatively the diffusion behavior of these elements during annealing; this can be done at the nanometre scale using analytical scanning transmission electron microscopy (STEM) of cross-sectional samples.

2. Experimental

Single layer rhombohedral PZT (of atomic ratio [Zr]/[Ti] = 65/35) films were prepared with 10 mol% excess Pb by a diol route. This composition was selected since it has been reported that PZT diol films normally crystallise into a (111) preferred orientation which is the direction of spontaneous polarisation of the rhombohedral phase.[12] Details of the sol preparation procedure have been reported elsewhere.[12] Films were deposited on platinised silicon substrates supplied by GEC-Marconi Technology. The configuration of the substrates was $Pt(111)/Ti/SiO_2/Si$, in which the Pt thickness was nominally 100 nm; the Ti layer 5 nm; the thickness of the SiO_2 layer was 360 nm and the total thickness of the substrate was ca. 1.5 mm. Si-based substrates were single crystal and (100) oriented, while Pt electrodes were polycrystalline with a (111) heteroepitaxial orientation.

As-deposited films were prefired at low temperatures (ca. 450–500°C) for 1 min before finally being fired at 700°C for 15 min by directly inserting the sample into a pre-heated tube furnace (approximate heating rate = 200°C min^{-1}). The firing temperature was recorded using a thermocouple placed next to the sample. The low temperature anneal was performed on a hotplate and generally it was difficult to ascertain the exact temperature experienced by the thin film sample.[13,14] For the samples reported here, a thermocouple placed on the surface of the hotplate gave a reading of 420°C although problems with poor thermal contact and heat-loss to the surroundings most probably led to an underestimate of the exact temperature. Current studies now rely on a thermocouple inserted into a copper block placed on the hotplate on which the sample is heated;[14] interpolation of results from this more accurate measurement method imply, for the results reported here, that the true temperature of the surface on which the substrate was placed was between 450 and 500°C.

TEM cross-sections were prepared using standard techniques,[15] these samples were dimpled and subsequently low angle ion beam thinned to electron transparency. Phase identification and microstructural observations were carried out using both XRD and TEM. XRD was performed on a Phillips ADP700 using Cu K_α radiation. TEM/STEM was performed on a Phillips CM20 operated at 200 kV and fitted with a LaB_6 source and an ultra thin window EDX detector (Oxford Instruments) and (Gatan 666) PEELS. High spatial resolution microanalysis was undertaken on a VG HB 501 dedicated STEM operated at 100 kV and fitted with UTW EDX (Tracor) and (Gatan) PEELS; this latter machine possesses a cold field emission source giving a usable analytical probe size of 1 nm together with a high current density. Beam broadening effects will degrade the ultimate spatial resolution fo microanalysis, particularly for the case of EDX where, even for a 1 nm probe, the actual resolution would be greater than 10 nm in regions containing heavy elements.

The diffusion behavior of each element was monitored by STEM/EDX line scans, which were susequently confirmed by EELS and EDX point analyses. EDX spectra were quantified using the Cliff–Lorimer technique, using k factors obtained from the virtual standards pack supplied with the Noran software and an absorption correction based on thicknesses determined by EELS. Pt L, Pb L, Zr L, Ti K and Si K lines were used for analysis. Considerably inaccuracies in Zr levels were obtained using Zr K lines presumably due to an inaccurate k factor, thus the Zr L line was used although it overlaps with Pb M which was removed for the purposes of quantification. EELS spectra were processed and quantified using Gatan EL/P software. Preliminary studies of local coordinations and valence states of atomic species were undertaken via analysis of the electron energy loss near edge structure (ELNES) associated with each EELS ionization edge.

3. Results and discussion

3.1. Low temperature prefired films

Fig. 1 shows a cross-sectional bright field image of the PZT film coated on the platinised Si substrate after the low temperature (ca. 450–500°C) prefiring treatment.

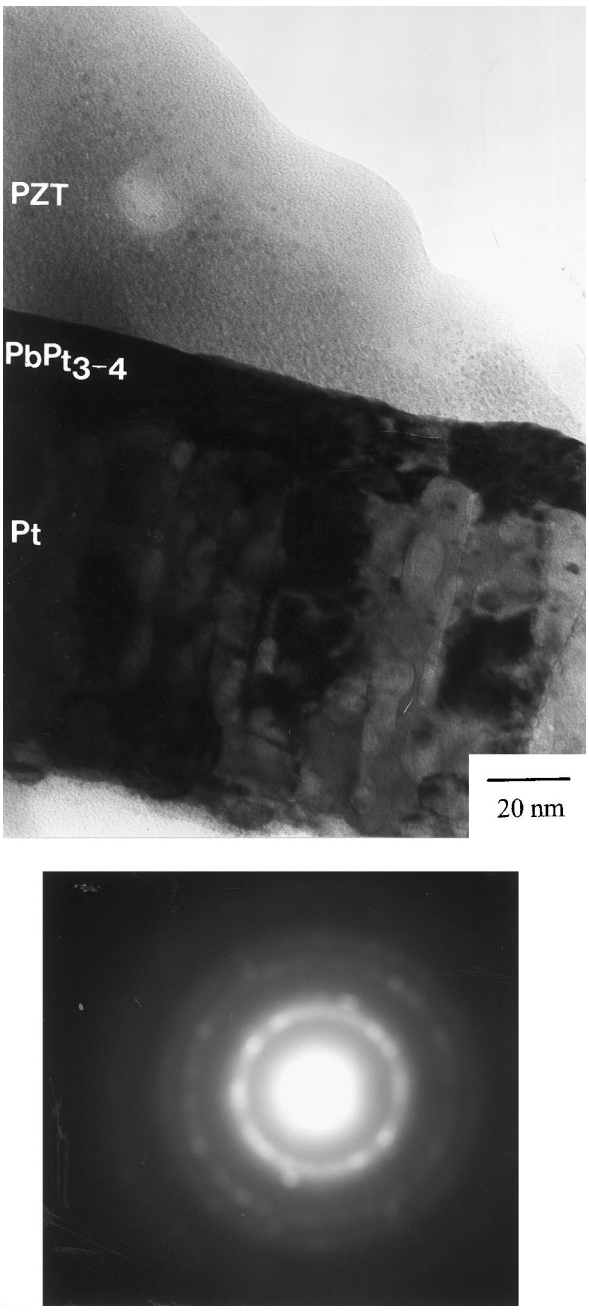

Fig. 1. TEM bright field image and SAED pattern of the prefired PZT film.

The selected area electron diffraction (SAED) pattern of the PZT layer (inset in Fig. 1) reveals a diffuse ring pattern indicating its general amorphous nature. EDX point analyses obtained from the PZT region near the Pt/PZT interface (Fig. 2a) showed anomalous amounts of Pb and Si as compared to the remainder of the film (Fig. 2b). EELS spectra of the Ti $L_{2,3}$- (Fig. 3a) and O K-edges (Fig. 3b) from the PZT layer gave a [Ti]/[O] atomic ratio of ca. 0.15 as compared to the expected ratio of ca. 0.12 for the original composition. The O K-edge ELNES (Fig. 3b) from the PZT layer is rather broad and featureless indicating the amorphous nature

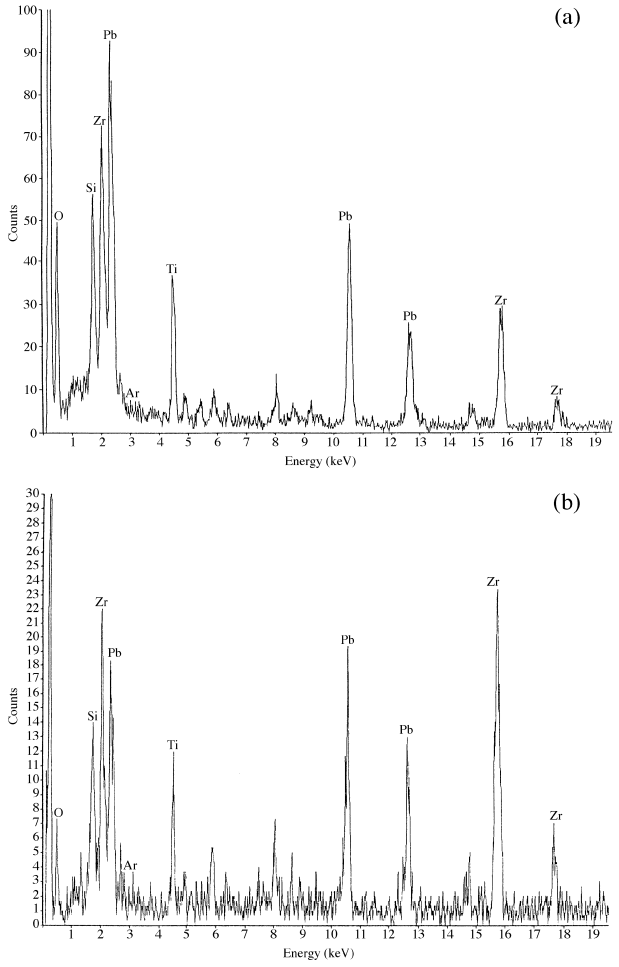

Fig. 2. EDX analyses of the prefired PZT film, (a) a region close to the Pt electrode and (b) a region further away from the Pt electrode.

of the film and this is confirmed by the small octahedral crystal field splitting observed on both the Ti L_3- and L_2- edges (Fig. 3a).[16]

The Pt electrode, shown in Fig. 1, exhibits diffraction contrast from the presence of polycrystalline, columnar grains, while at the film/substrate interface there exists a dark layer with a rather uniform thickness of ca. 20–25 nm. EDX analysis indicated that this interfacial layer was composed of a substantial amount of Pb, Pt and Si (Fig. 4). This observation is in good agreement with the findings of XRD (Fig. 5a) which indicated the presence of an extra phase at $2\theta = 38.57$. Quantitative analysis of 10 EDX spectra obtained from different regions along the interface layer gave a [Pt]/[Pb] atomic ratio of between 3 and 4. Therefore the Pt/PZT interface phase was assigned as $PbPt_{3-4}$. These independent results, first reported in Ref. 13, are in agreement with recent results reported by Huang et al.[17–19] who observed a $PbPt_3$ interphase after annealing at 440°C. Selected area electron diffraction (SAED) patterns (Fig. 6c) obtained from the $PbPt_{3-4}$ and Pt regions show that the $PbPt_{3-4}$ grew epitaxially on the Pt electrode with a (111) preferred

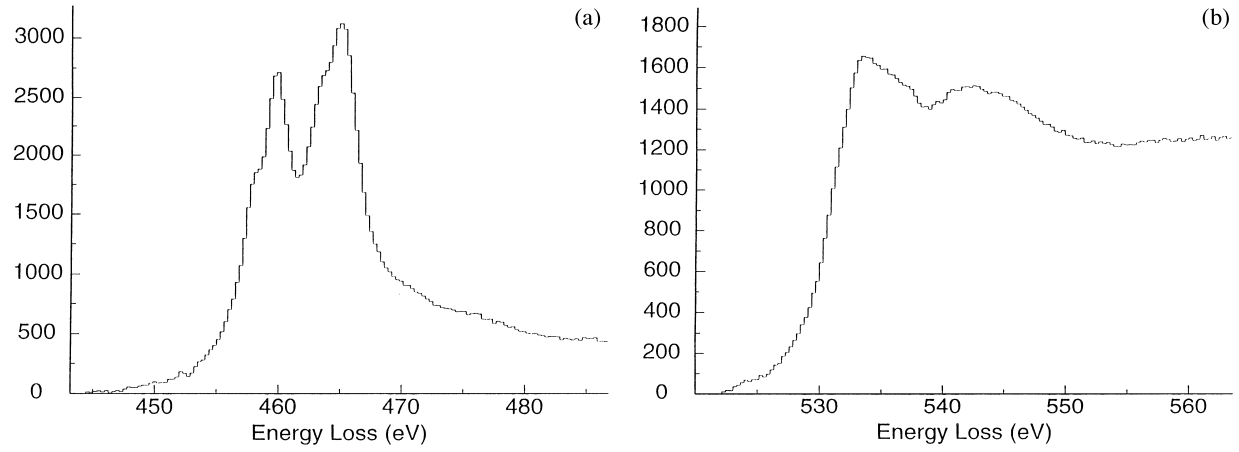

Fig. 3. EELS spectra of the prefired PZT layer, (a) the Ti $L_{2,3}$-edge and (b) O K-edge.

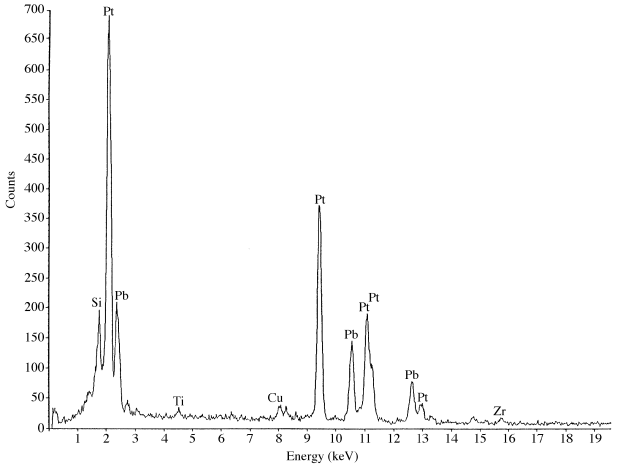

Fig. 4. EDX analysis obtained from the $PbPt_x$ interface layer in the prefired film.

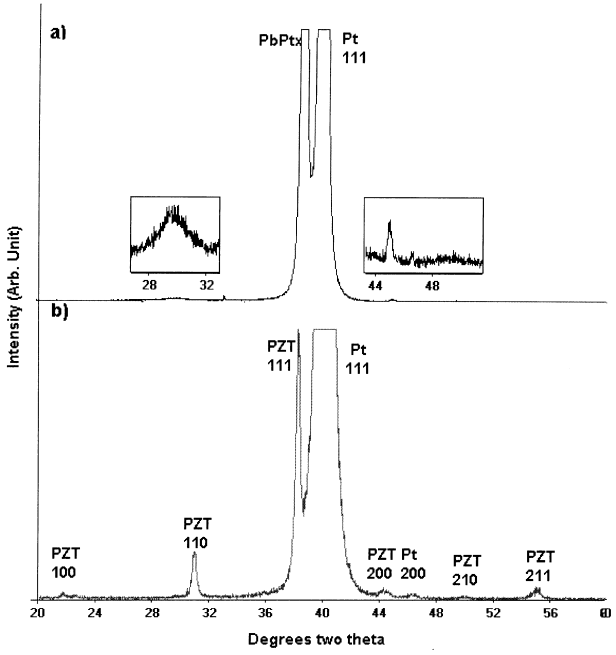

Fig. 5. XRD trace of (a) the prefired PZT film and (b) the PZT film after both prefiring and annealing at 700°C.

orientation. This interpretation was confirmed by microdiffaction patterns obtained from the $PbPt_{3-4}$ (Fig. 6a) and the Pt region (Fig. 6b). EDX analysis from the middle of the Pt electrode did not show a significant interdiffusion of the film and substrate elements; only small amounts of Ti and Si being observed at this position. This implies that no substantial migration of elements between the film and substrate had occurred except in the regions neighbouring the PZT layer, where substantial diffusion of Pb into the Pt layer had occurred.

A high level of oxygen in the Ti layer could be detected by both EDX (Fig. 7) and EELS suggesting that Ti was probably oxidised and had formed TiO_2. This has been observed in previous studies.[20] The source of the oxygen has not been determined, however, it has been reported that migration of oxygen could occur from either the free surface of the thin film or the SiO_2 layer.[21] Small amounts of Si and Pt were also detected in this oxidised Ti layer.

Diffusion of these elements was further confirmed by EDX linescans, obtained by sequentially stepping the beam from the SiO_2 layer into the Pt layer (Fig. 8) as well as from the Pt layer into the PZT layer (Fig. 9), of the cross-sectional samples after low temperature prefiring. A gradual interdiffusion of Pt and Ti was observed (Fig. 8a and c). Diffusion of Pb into the Pt layer (Fig. 9b), and also into both the Ti and SiO_2 layers (Fig. 8b), with a slight build up at the Pt/Ti interface, was also apparent. At the Pt/PZT interface, a step in the Pt and Pb concentration was observed (Fig. 9a and b), here the concentration of Pt was reduced as compared to the Pt substrate region. This is additional evidence

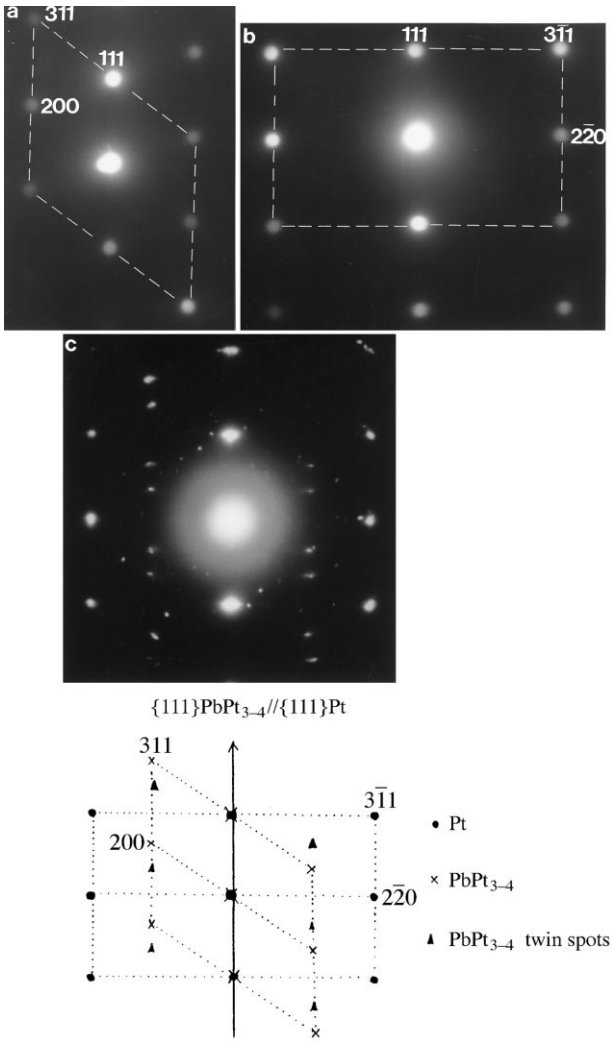

Fig. 6. Electron diffraction of the prefired film, (a) microdiffraction pattern obtained from the $PbPt_{3-4}$ phase, (b) microdiffraction pattern obtained from the Pt electrode and (c) SAED pattern obtained from both the Pt and $PbPt_{3-4}$ regions.

for formation of the $PbPt_{3-4}$ reaction interphase described above.

Surprisingly, a dramatic outward diffusion of Si into both the Ti and Pt layers (Fig. 8e) as well as further into the PZT layer was observed, with a small decrease at the Ti/Pt interface. This could have occurred: (a) during the low temperature prefiring stage, (b) during storage, or, (c) during the TEM sample preparation. Further work is required to resolve this point.

3.2. High temperature annealed films

Fig. 10 shows the TEM bright field image obtained from a film which had been prefired at low temperatures and finally fired at 700°C for 15 min. The PZT film showed the formation of small columnar grains, which were ca. 0.1–0.2 μm in lateral diameter and ca. 0.3 μm in length. These appeared to have grown from the bottom

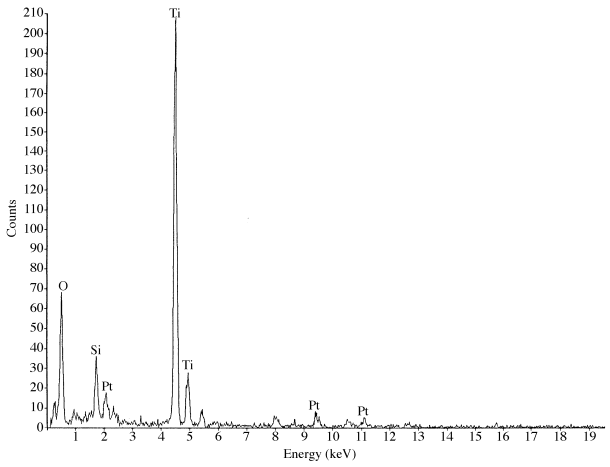

Fig. 7. EDX analysis of the Ti buffer layer in the prefired film.

electrode, through the bulk of the film towards the top surface (marked as 'i').

In the micrograph in Fig. 10a, the growth of the columnar grains appears to have been hindered by a large area of an apparently nanocrystalline phase which had originated at the top surface and grew larger through the bulk film (marked as "ii"). However, the nanocrystalline phase was not only found to be at the top surface but sometimes was apparent within the bulk film as a pocket between larger grains (seen on the right hand side of Fig. 10b). In the literature, this nanocrystalline phase has been reported to be Pb-deficient and is generally referred to as a pyrochlore or fluorite-type phase. On the top surface, in the absence of this nanocrystalline phase, large grains ca. 0.3–0.4 μm in lateral diameter were observed (marked as 'iv' in Fig. 10a).

XRD of this sample showed that PZT had crystallized with a (111) preferred orientation, no other phase was apparent (Fig. 5b). SAED analysis of the orientation relationship between the bottom electrode and the PZT film was difficult since both the Pt electrode and PZT film were polycrystalline and interference from neighbouring grains was problematic. However, the columnar grains which nucleated from the bottom Pt electrode and were a major part of the PZT film were tentatively assigned as growing along the ⟨111⟩ PZT direction, while the surface grains which were larger in lateral size appeared to be randomly oriented.

An SAED pattern (Fig. 11) obtained from the so called 'pyrochlore' phase indicates its nanocrystalline nature. The measured d-spacings and tentative lattice parameters of this phase together with the d-spacings of the pyrochlore phase for PZT (53/47) reported in literature[22–24] are given in Table 1; note there are problems with the lattice parameter value reported by Lakeman et al.[23] based on their corresponding fluorite-type d spacings. The d-spacing values obtained in this study are different from previous studies, which is

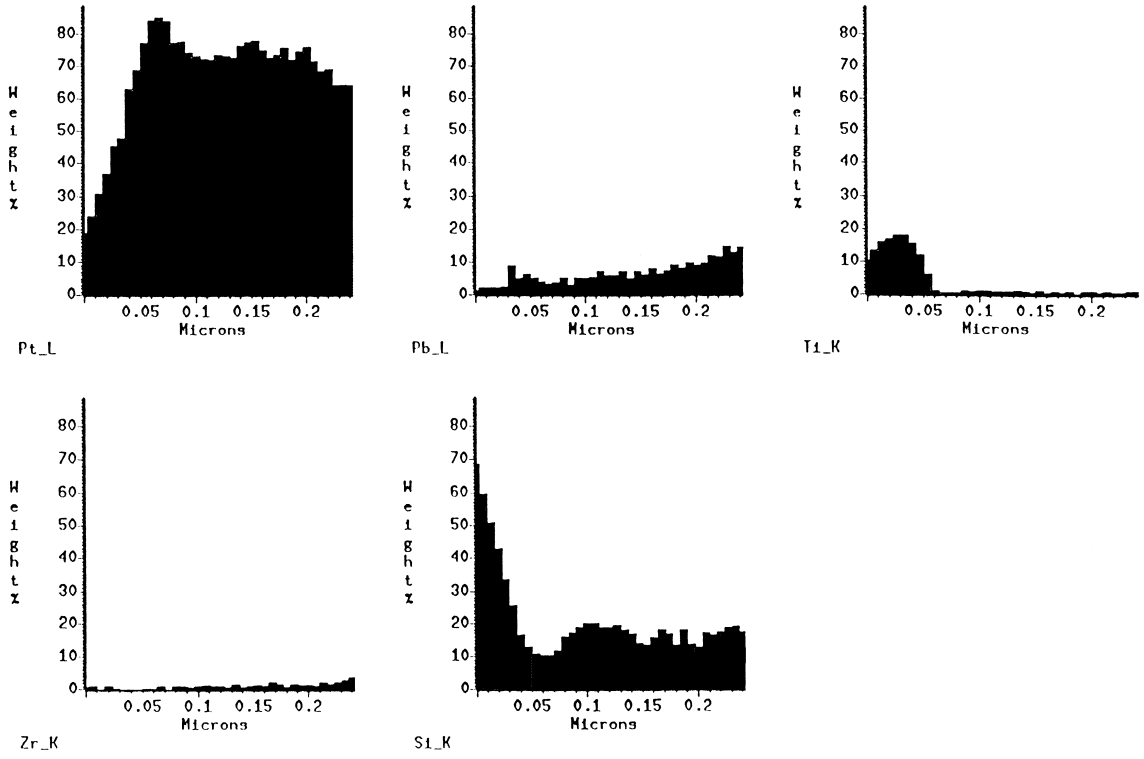

Fig. 8. Quantitative EDX linescans obtained from the SiO_2 layer (LHS) into the Pt layer (RHS) in the prefired film. The SiO_2/Ti/Pt interface is at ca. 0.06 μm on the *x*-axis.

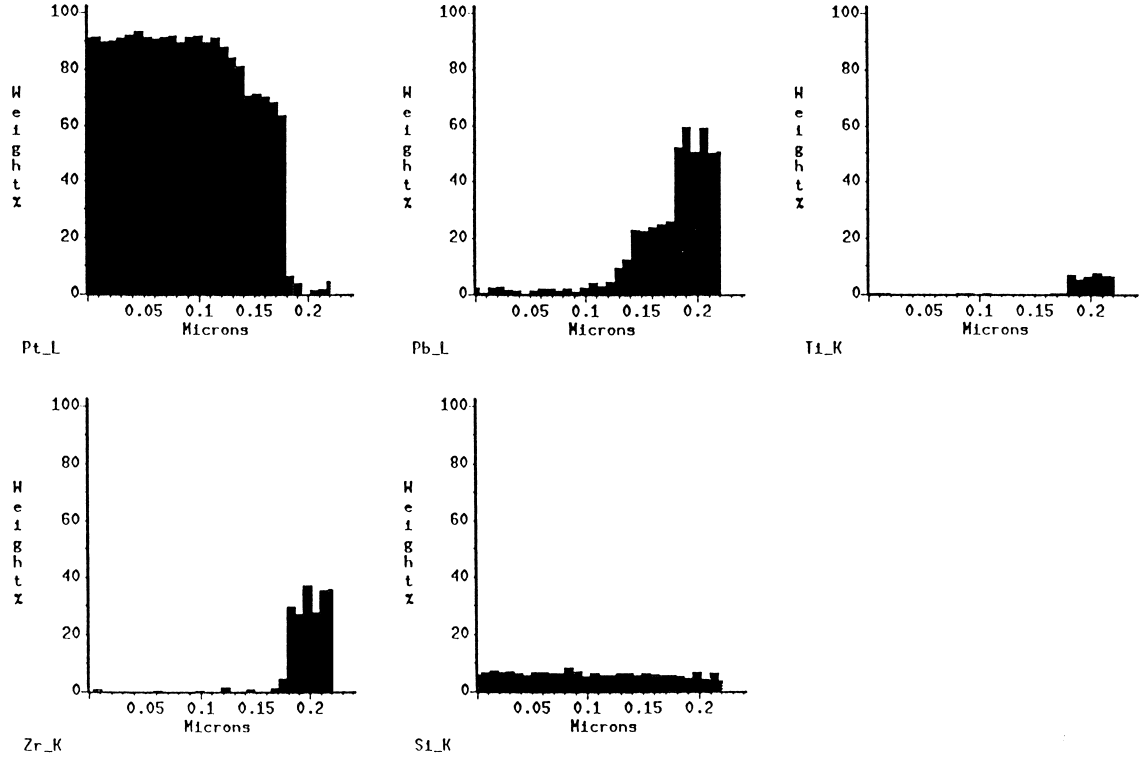

Fig. 9. Quantitative EDX linescans obtained from the Pt layer (LHS) into the PZT layer (RHS) in the prefired film. The $PbPt_{3-4}$ reaction interphase is situated between ca. 0.145 and 0.175 μm on the *x*-axis.

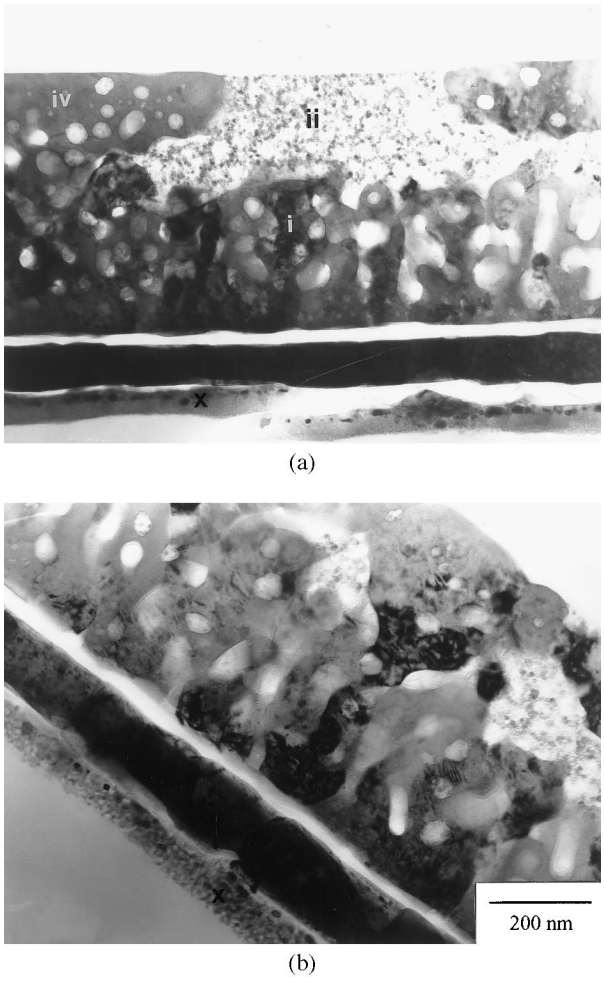

Fig. 10. (a) TEM bright field image of the PZT film after both prefiring and annealing at 700°C for 15 min; (b) TEM bright field image of the PZT film after both prefiring and final firing showing a nanocrystalline pocket.

probably due to the different chemical compositions of the films (the [Zr]/[Ti] atomic ratio in this study is 65/35 while it was 53/47 in most previous studies).

The actual structure of this nanocrystalline phase is somewhat contentious. It has long been believed that the Pb-deficient nanocrystalline phase occurring in the PZT system has a structure similar to the mineral pyrochlore which is based on a 3-D network of corner sharing BO_6 octahedra. However, some authors, for instance Wilkinson et al.[22] and Lakeman et al.,[23] have reported that the nanocrystalline phase may have a fluorite structure rather than the 3-D network of corner sharing BO_6 octahedra. This suggestion was based on the absence of superlattice reflections in diffraction data, as well as on the tendency for Zr to adopt a co-ordination number higher than 6. Based on the fact that the pyrochlore structure, which contains corner sharing BO_6 octahedra, has a higher symmetry than the fluorite structure and can be distinguished by the existence of d_{311} and d_{111} cell doubling reflections in the SAED pattern,[22,23]

Fig. 11. SAED pattern obtained from the nanocrystalline phase in the annealed film.

Table 1
Comparison of lattice parameters calculated from SAED patterns based on cubic pyrochlore and fluorite structures

Wilkinson et al.[22] fluorite (a = 5.25 Å)	Kwok and Desu[24] pyrochlore (a = 10.48 Å)	Lakeman et al.[23] (a = 5.1 Å)	This study (a = 5.02 Å)
	d_{111} = 6.04 Å		
	d_{311} = 3.16 Å		
d_{111} = 3.03 Å	d_{222} = 3.03 Å	3.03 Å	2.97 Å
d_{200} = 2.63 Å	d_{400} = 2.62 Å	2.62 Å	2.51 Å
d_{220} = 1.86 Å	d_{440} = 1.85 Å	1.85 Å	1.80 Å
d_{311} = 1.58 Å	d_{622} = 1.58 Å	1.58 Å	1.54 Å

the nanocrystalline phase observed in this study can therefore be identified as possessing a fluorite structure due to the absence of these reflections.

EDX spectra obtained from the nanocrystalline phase (Fig. 12a) indicated a considerably Pb-deficient, and Zr-rich condition as compared to the EDX spectra obtained from the area neighbouring the nanocrystalline phase (Fig. 12b). General EDX analysis of the PZT layer also shows a significant amount of Si. The nanocrystalline phase was assigned as the Zr-rich nanocrystalline fluorite phase while the Pb-rich, Zr-deficient phase was assigned as the PZT phase. The compositional analyses (in atomic ratios) were as follows:

Nanocrystalline fluorite phase: [Pb]:[Zr]:[Ti] = 34:50:16
PZT phase: [Pb]:[Zr]:[Ti] = 65:13:23

Note these values are very different from the desired target composition of [Pb]:[Zr]:[Ti] = 50:32.5:17.5.

EELS spectra from the PZT phase gave a [Ti]/[O] atomic ratio of 0.16 similar to that obtained from the amorphous PZT film which had been prefired. However, the O K-ELNES from the PZT phase (Fig. 13a) was typical of a crystalline perovskite structure[25] and the Ti $L_{2,3}$-edge (Fig. 13b) also exhibited a larger crystal field splitting than that of the amorphous PZT (Fig. 3a) also indicative of a crystalline structure. The [Ti]/[O] atomic ratio from the nanocrystalline phase or Pb-deficient region was only 0.07 and exhibited a significantly different O K-ELNES (Fig. 13a) and Ti $L_{2,3}$-octahedral field splitting (Fig. 13b) from the PZT phase. The O K-ELNES from this region is similar to that observed in cubic zirconia[26] which has a fluorite-type structure and these changes are therefore consistent with the conclusions drawn from the electron and X-ray diffraction data.

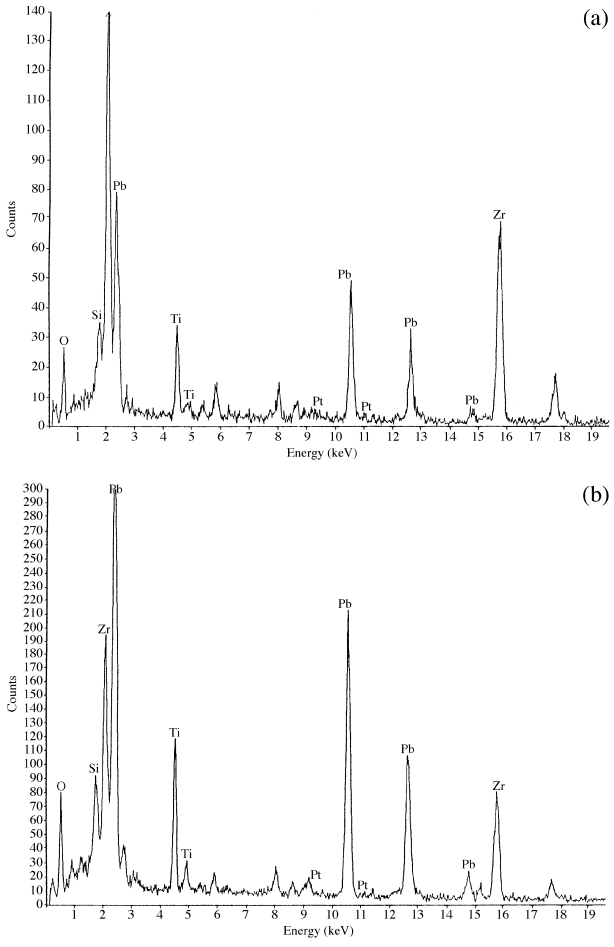

Fig. 12. EDX analysis of (a) the nanocrystalline phase and (b) an area neighbouring the nanocrystalline phase in the annealed sample.

EDX point analyses of the Pt layer neighbouring the Ti layer showed a significant amount of Si, Ti and Pb in this layer (Fig. 14a). However, the levels of Ti and Pb were considerably reduced in the middle of the Pt layer (Fig. 14b). EDX spectra from the Pt layer at the PZT/Pt interface region showed almost entirely Pt with a small amount of Si (Fig. 14c). Thus, the distinct 20 nm thick $PbPt_{3-4}$ phase was no longer present following high temperature firing.

In the Ti layer, substantial amounts of oxygen were again detected by both EDX and EELS, suggesting that the Ti had oxidised to form TiO_2. EELS spectra (Fig. 15) gave a [Ti]/[O] atomic ratio of 0.45 and an O K-edge structure characteristic of TiO_2. Small amounts of Si, Pt and Pb were also detected in this layer by EDX.

EDX analyses of the SiO_2 layer did not show significant contamination from other elements. However, at the boundary between the Ti and SiO_2 layers, there existed a distinct Pb-rich layer (marked as as 'x' in Fig. 10a and b) and an EDX spectrum of this phase is shown in Fig. 16. This analysis suggests that further diffusion of Pb to the underlying layers occurs after firing at the

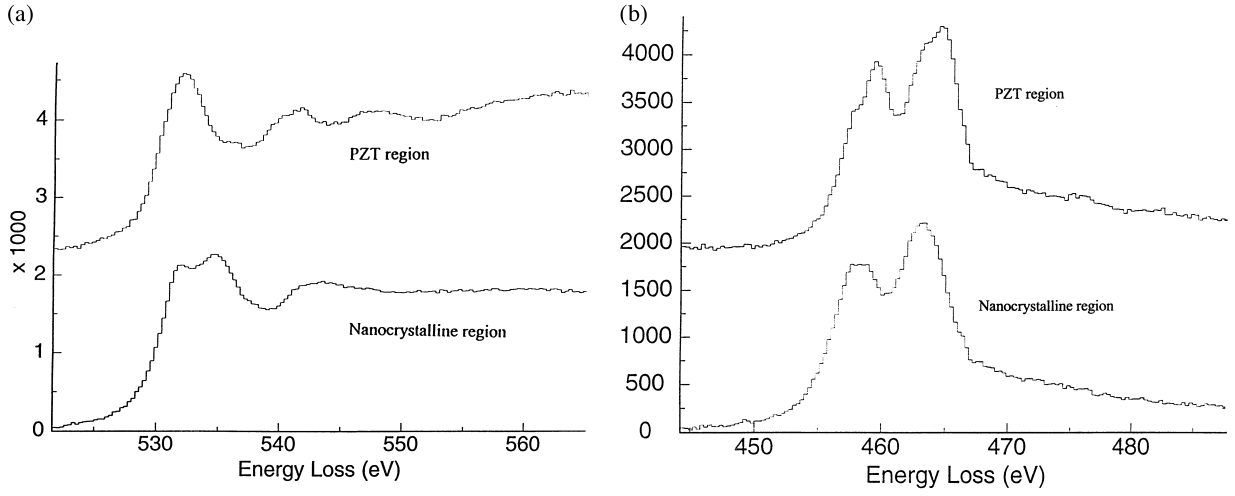

Fig. 13. (a) O K-ELNES obtained from the PZT region and the nanocrystalline region in the annealed sample, (b) Ti $L_{2,3}$-ELNES obtained from the PZT region and the nanocrystalline region in the annealed sample.

higher temperature. Therefore the disappearance of the $PbPt_{3-4}$ phase after firing at 700°C may be due to the severe diffusion of Pb down to the bottom layers rather than its re-oxidation to Pb^{2+} as reported by Chen and Chen.[6]

A quantitative EDX line scan performed across the film thickness from the PZT layer to the SiO_2 layer is shown in Fig. 17. The diffusion of Ti from the Ti layer into the Pt layer was clearly observed (Fig. 17a). There appeared to be a step in both the Ti and Pt concentrations which may correspond to a Pt–Ti reaction interphase; however, substantial Si also appears to be involved in this reaction product. Pt appears to have diffused slightly towards the top surface, i.e. towards the PZT layer, and, more significantly, towards the underlying Ti and SiO_2 layers (Fig. 17b). A substantial amount of Pb was observed in the Ti and SiO_2 layers while only a small amount remained in the Pt layer (Fig. 17c) suggesting that Pb had progressively diffused down to the Ti and SiO_2 layers upon high temperature firing. No significant diffusion of Zr to the underlying electrode was observed (Fig. 17d). Conversely outward diffusion of Si to the PZT layer was clearly observed (Fig. 17e) as in the low temperature prefired sample.

Whether the diffusion of Pb to the underlying layers was the only cause of Pb loss is not yet confirmed, since it has generally been reported that the Pb-deficiency in

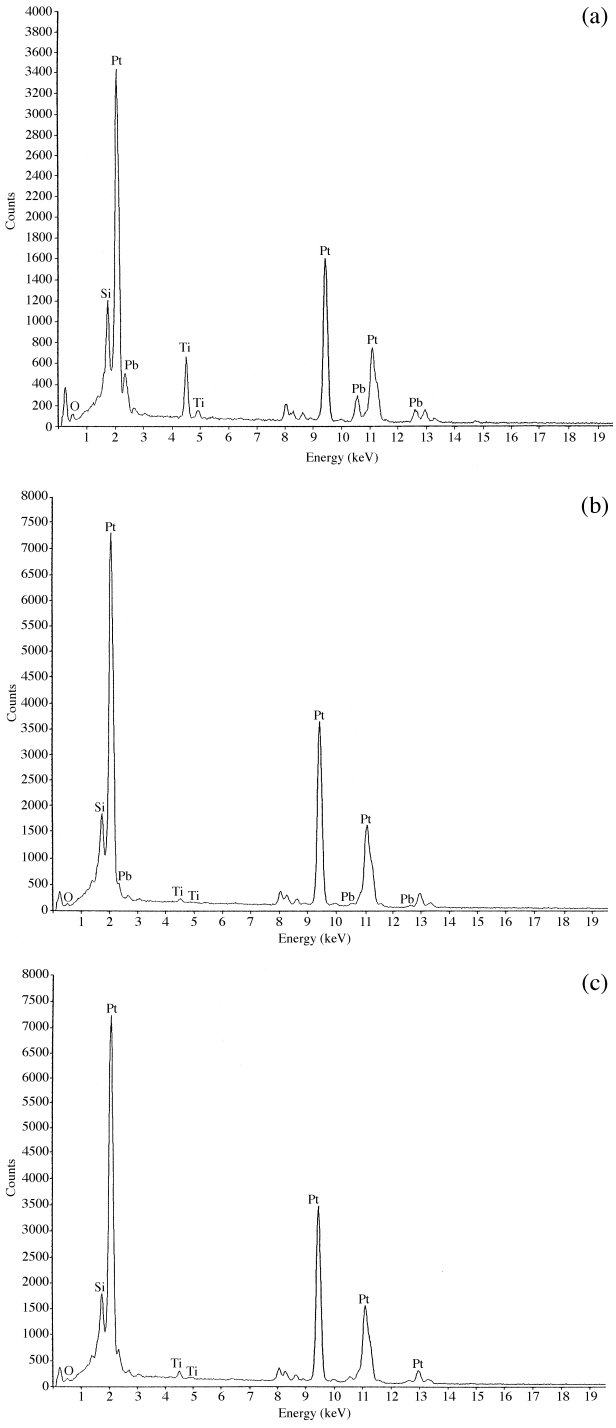

Fig. 14. EDX analysis of (a) the Pt layer neighbouring the Ti layer, (b) the middle of the Pt layer and (c) the PZT/Pt interface region in the annealed sample.

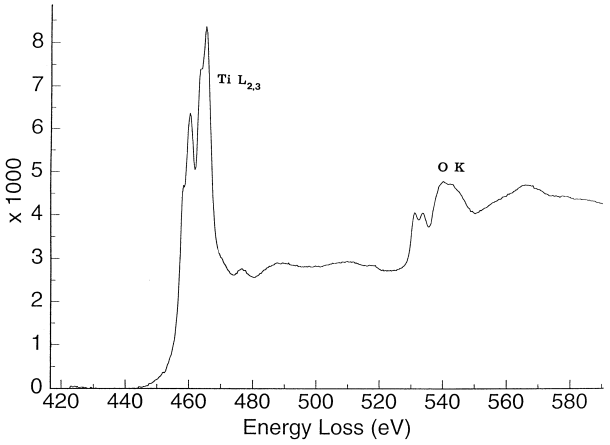

Fig. 15. EELS spectrum of the Ti buffer layer in the annealed sample.

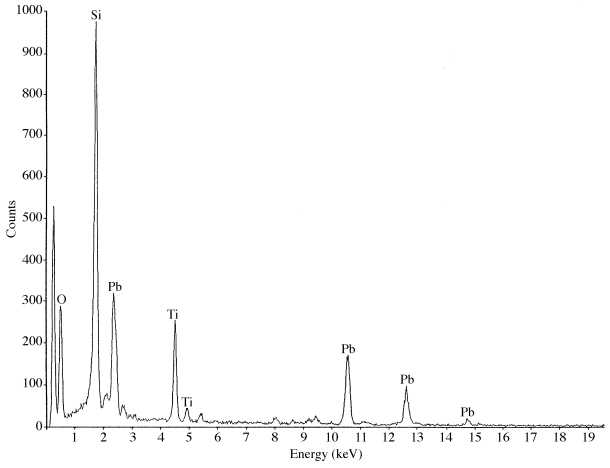

Fig. 16. EDX analysis of the Pb-rich interface layer in the annealed sample.

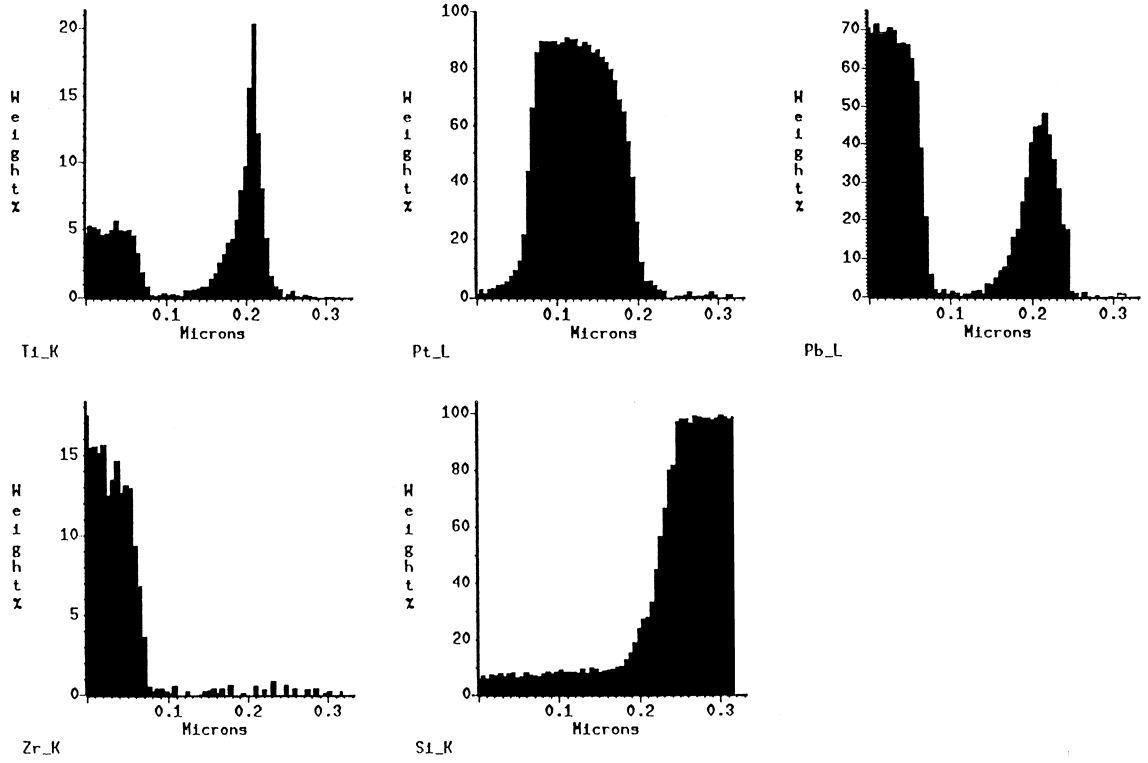

Fig. 17. Quantitative EDX linescans from the PZT layer (LHS) into the SiO_2 layer (RHS) in the annealed sample. The PZT/Pt interface is at ca. 0.7 μm on the *x*-axis, while the Pt/Ti/SiO_2 interface is at ca. 0.19 μm.

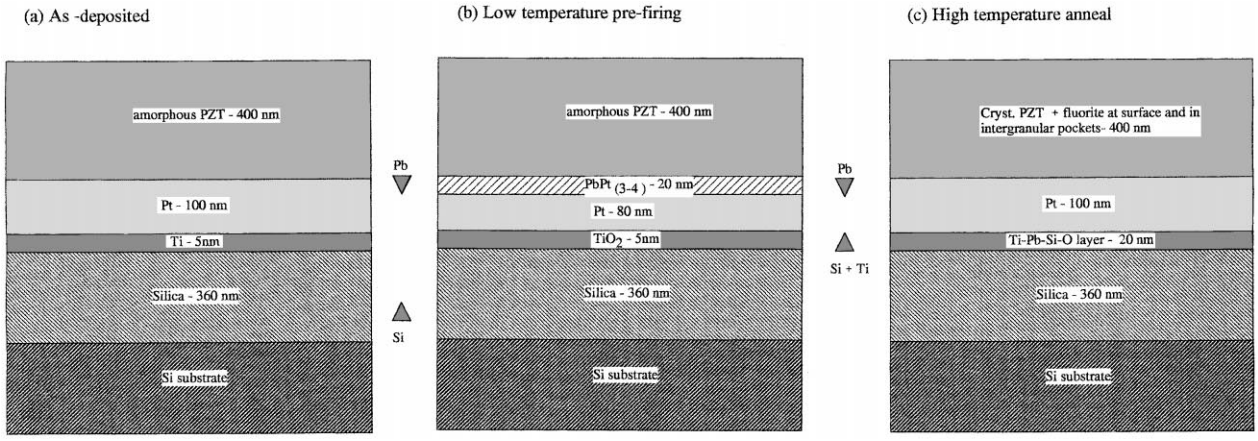

Fig. 18. Schematic diagram of the microstructural changes occuring during sol–gel thin film processing: (a) as deposited, (b) after low temperature pre-firing and (c) after high temperature annealing.

PZT is due to the volatility of PbO.[27] Further work is needed to clarified this point.

3.3. General discussion

A summary of the microstructural observations in shown schematically in Fig. 18. It has been evident from our investigation that diffusion of both film and substrate elements occurs even when heating at comparatively low temperatures for short times. Diffusion of Pb to the Pt layer at the pre-firing stage results in the formation of a $PbPt_{3-4}$ phase which grows epitaxially on the Pt layer. These findings are in agreement with recent data of Huang et al.[17–19] The presence of this intermediate phase has been thought to be the reason for the development of (111) texture in deposited PZT films since the $PbPt_x$ growing epitaxially in a (111) orientation serves as the nucleation sites for the films due to the small lattice mismatch (ca. 0.4%) with the PZT(111). Firing the film at 700°C for 15 min results in more

severe diffusion of Pb to the underlying layers and forms a distinct Pb–Ti–Si–O layer at the Ti/SiO_2 interface.

Formation of either a Pt_3Ti or a TiO_x phase at the prefiring stage appears unlikely under the present conditions, since the outward-diffusion of Ti to the surface of the Pt layer was not detected at this stage. Diffusion of Ti into the PZT layer becomes noticeable only after firing the film at 700°C for 15 min. These results have been confirmed by XPS analyses of the surface composition of $Pt/SiO_2/Si$ substrates following various heat treatments.[28]

Significant levels of Si diffusion into the PZT layer were observed even after the prefiring stage. This suggests the inability of the Ti layer to prevent the outward diffusion of Si into the PZT layer. However, it is possible that severe outward diffusion of Si had occurred prior to heating and during storage of the substrate, alternatively it could be simply an artifact of TEM sample preparation, although present dynamic SIMS measurements seem to confirm that the severe outward diffusion of Si is indeed present in the bulk thin film specimen following heat treatment.[28]

4. Conclusions

TEM-based microstructural investigations of elemental interdiffusion between PZT(65/35) diol films and $Pt/SiO_2/Si$ substrates has been performed. Under ambient firing conditions, the following observations were made:

1. Severe diffusion of Pb into the underlying substrate could be observed in both the low temperature prefired film and the 700°C annealed film. Diffusion of Pb into the underlying Pt electrode during prefiring results in the formation of a $PbPt_x$ interphase layer. This interfacial layer, which is believed to serve as nucleation sites for columnar PZT crystals, was estimated to have a formula $PbPt_{3-4}$. However, further diffusion of Pb into the underlying Ti and SiO_2 layers was observed in the 700°C annealed film and caused the $PbPt_{3-4}$ phase to disappear. Pb appears to react with Si and Ti at the SiO_2/Ti interface to form a reaction product of unknown stoichiometry and structure.
2. No diffusion of Zr was detected in both the prefired film or the 700°C annealed film indicating the inert nature of this element.
3. Oxidation of Ti in the Ti layer to form TiO_2 was observed in both the prefired film and the 700°C annealed film. Outward diffusion of Ti from the Ti layer into the PZT layer was clearly seen in the film after firing at 700°C whilst this diffusion was not significant in the prefired film.
4. Possible outward diffusion of Si to the Pt and PZT layers was observed in both the prefired film and the 700°C annealed film.
5. The diffusion observed in this study was a time–temperature dependent process, i.e. it increased as the layers were heated to higher temperatures and for longer times, such as the diffusion of Pb into the underlying substrate.
6. The PZT film prefired at low temperature (ca. 450–500°C) was amorphous before finally changing to the perovskite structure at 700°C. This transformation was associated with the formation of a nanocrystalline phase.
7. EELS spectra indicated that the intermediate nanocrystalline phase observed in the 700°C annealed PZT film had a different structure and stoichiometry from the Pb-rich phase which was assigned as the PZT phase. Neither of these phases possessed a cation stoichiometry close to that of the desired target composition. The nanocrystalline phase was a Pb-deficient, Zr-rich phase and exhibited a fluorite structure as determined from the SAED pattern. The existence of the nanocrystalline phase after annealing at high temperature confirmed that the incorporation of 10% excess Pb incorporation was insufficient to compensate for the lead loss possibly due to diffusion into the substrate during the high temperature firing.

Acknowledgements

DK, TC and MK all acknowledge support from the Thai Government during the course of their study. RB is extremely grateful to Max-Planck-Institut Stuttgart for access to STEM facilities.

References

1. Fox, G. R., Trolier-McKinstry, S., Krupandhi, S. B. and Casas, L. M., *J. Mat. Res.*, 1995, **10**, 1508.
2. Hwang, C. S. and Kim, H. J., *J. Am Ceram. Soc.*, 1995, **78**, 337.
3. Kim, S. T., Kim, C. Y., Park, K. H., Kim, K. Y., Lee, J. S., Jeong, Y. W. and Kwon, H. J., *Jpn. J. Appl., Phys.*, 1995, **34**, 4945.
4. Sameshima, K., Nakamura, T., Hoshiba, K., Nakao, Y., Kamisawa, A., Atsuki, T., Soyama, N. and Ogi, K., *Jpn. Jn. Appl. Phys.*, 1992, **32**, 4144.
5. Brooks, K. G., Reaney, I. M., Klissurska, R., Huang, Y., Bursill, L. and Setter, N., *J. Mat. Res.*, 1994, **9**, 2540.
6. Chen, S. Y. and Chen, I. W., *J. Am Ceram. Soc.*, 1994, **77**, 2337.
7. Atsuki, T., Soyama, N., Sasaki, G., Yonezawa, T., Ogi, K., Sameshima, K., Hoshiba, K., Nakao, Y. and Kamisawa, A., *Jpn. J. Appl. Phys*, 1994, **33**, 5196.
8. Bursill, L. A. and Brooks, K. G., *J. Appl. Phys.*, 1994, **75**, 4501.
9. JCPDS: File Card No. 6-574.
10. JCPDS: File Card No. 33-784.
11. Tani, T. and Xu, Z., *Payne Mat. Res. Symp. Proc.*, 1993, **310**, 269.
12. Tu, Y. L. and Milne, S. J., *J. Mat. Res.*, 1995, **10**, 3222.
13. Kaewchinda, D., Ph.D. thesis, University of Leeds, 1998.

14. Naksata, M., unpublished work.
15. Lee, W. E. and Rainforth, W. M., *Ceramic Microstructures*. Chapman and Hall, London, 1994.
16. Brydson, R., Sauer, H. and Engel, W., in *Transmission EELS in Materials Science*. TMS, Warrendable PA, 1992 (Chapter 6).
17. Huang, Z., Zhang, Q. and Whatmore, R. W., *J. Mat. Sci. Lett*., 1998, **17**, 1157.
18. Huang, Z., Zhang, Q. and Whatmore, R. W., *J. Appl. Phys*., 1999, **85**, 7355.
19. Huang, Z., Zhang, Q. and Whatmore, R. W., *J. Appl. Phys*., 1999, **86**, 1662.
20. Sreenivas, K., Reaney, I., Maeder, T., Setter, N., Jagadish, C. and Elliman, R. G., *J. Appl. Phys*, 1994, **75**, 232.
21. Park, K. H., Kim, C. Y., Jeong, Y. W., Kwon, H. J., Kim, K. Y., Lee, J. S. and Kim, S. T., *J. Mater. Res*., 1995, **10**, 1790.
22. Wilkinson, A. P., Speck, J. S., Cheetham, A. K., Natarajan, S. and Thomas, J. M., *Chem. Mater*., 1994, **6**, 750.
23. Lakeman, C. D. E., Xu, Z. and Payne, D. A., *J. Mater. Res*., 1995, **10**, 2042.
24. Kwok, C. K. and Desu, S. B., *Appl. Phy. Lett*., 1992, **60**, 1430.
25. Brydson, R., Sauer, H., Engel, W. and Hofer, F., *J. Phys. Condensed Matter*, 1992, **4**, 3429.
26. McComb, D. W., *Phys. Rev. B*, 1996, **54**, 54.
27. Moulson, A. J. and Herbert, J. M., *Electroceramics: Materials, Properties and Applications*. Chapman and Hall, London, 1990.
28. Brydson, R., unpublished work.